Higher order cumulants of transverse momentum and harmonic flow in relativistic heavy ion collisions

Piotr Bożek [*] and Rupam Samanta [†]

Faculty of Physics and Applied Computer Science, AGH University of Science and Technology, aleja Mickiewicza 30, 30-059 Cracow, Poland

(Received 5 April 2021; revised 14 June 2021; accepted 6 July 2021; published 28 July 2021)

Higher order symmetric cumulants of global collective observables in heavy ion collisions are studied. The symmetric cumulants can be straightforwardly constructed for scalar observables: the average transverse momentum, the multiplicity, and the squares of harmonic flow vectors. Third and fourth order cumulants are calculated in the hydrodynamic model. A linear predictor of the average transverse momentum and harmonic flow coefficients in a collision is used to predict the values of the cumulants from the moments of the initial distribution. The symmetric cumulants divided by the averages (or the standard deviations) of the considered observables can be used as a fine tool to study correlations present in the initial state of the collision.

DOI: 10.1103/PhysRevC.104.014905

I. INTRODUCTION

The dense matter created in relativistic heavy ion collisions expands rapidly. The study of the collective flow of the expanding matter, modeled by the viscous hydrodynamics, can be used to study its properties [1–3]. One of the difficulties in this task lies in the uncertainty on the initial conditions for the hydrodynamic evolution. To reduce the uncertainty in the prediction of the harmonic flow coefficients, a number of additional observables based on correlators involving four or more particles have been proposed to constrain the initial conditions.

The expansion in the directions transverse to the beam direction generates the collective transverse flow. Of particular importance are the harmonic coefficients of the azimuthal particle distribution reflecting the azimuthal asymmetry of the initial conditions. The average transverse momentum of particles emitted in a collision is a measure of the overall radial expansion. The final transverse momentum is related to the size of the initial source [4]. Events with a smaller size of the interaction region have larger energy density gradients and a larger transverse push is formed in the expansion. The scaled transverse momentum fluctuations reflect, in the first approximation, the fluctuations of the initial size and in the entropy deposition.

A finer tool to look at the correlations of the collective flow observables in heavy ion collisions is given by the correlation coefficient $\rho(p_T, v_n^2)$ between the average transverse momentum p_T and the harmonic flow coefficient v_n^2 in an event [5]. The correlation of the elliptic or triangular flow with the average transverse momentum is well described by the correlations present in the initial state of the hydrodynamic evolution [6–8]. Thus, the correlation coefficient of transverse momentum p_T and the elliptic or triangular flow coefficient can serve as a tool to study correlations present in the initial state. The correlation coefficient has been measured for Pb + Pb and p + Pb collisions by the ATLAS Collaboration [9]. The experimental data on $\rho([p_T], v_2^2)$ in Pb + Pb collisions are qualitatively well described by hydrodynamic models. However, the magnitude and the sign of the correlation coefficient $\rho([p_T], v_3^2)$ are not well described in most of the calculations.

The study of the correlation coefficient between transverse momentum and elliptic flow is particularly interesting in deformed nuclei. In central collisions of deformed nuclei the orientation of the colliding deformed nuclei leads to specific correlations between the initial size and the elliptic deformation [10,11]. Experimental results show a sensitivity of the correlation coefficient $\rho([p_T], v_2^2)$ to the nuclear deformation [12,13]. The transverse momentum-harmonic flow correlation coefficient in peripheral events can be sensitive to initial momentum correlation that would survive the hydrodynamic evolution [14].

In this paper we explore higher order correlators of the harmonic flow and of the average transverse momentum. We study higher order symmetric cumulants [15–17] of scalar quantities: the transverse momentum, multiplicity, and the squares of harmonic flow vectors of different order. We present predictions for the third and fourth order normalized symmetric cumulants for collisions of spherical Pb + Pb and deformed U + U nuclei in the hydrodynamic model. We propose two different ways to normalize the higher cumulants, by the average or by the standard deviations of the observables taken in the cumulant. The calculations are compared to the results obtained using a linear predictor based on moments of the initial density. The higher order cumulants calculated in the hydrodynamic model could be measured experimentally.

[*] piotr.bozek@fis.agh.edu.pl
[†] rsamanta@agh.edu.pl

II. CORRELATIONS OF GLOBAL OBSERVABLES IN AN EVENT

A. Model

Expanding the azimuthal dependence of particle distributions in Fourier series we can write

$$\frac{dN}{dpd\phi} = \frac{dN}{2\pi dp}\left(1 + 2\sum_{n=1}^{\infty} V_n(p)e^{in\phi}\right), \tag{1}$$

using the complex plane notation for the transverse plane (p, ϕ). In this paper we use boost invariant calculations and the results should be compared to experimental results obtained at central rapidities in heavy ion collisions. Both the transverse momentum distribution $\frac{dN}{dp}$ and the harmonic flow vectors V_n fluctuate event by event. In this paper we study event by event correlations between moments of the distribution $\frac{dN}{dpd\phi}$ integrated in a range of transverse momenta, the charged particle multiplicity

$$N = \int_{p_{\min}}^{p_{\max}} dp \frac{dN}{dp}, \tag{2}$$

the average transverse momentum in an event

$$p_T = \frac{1}{N}\int_{p_{\min}}^{p_{\max}} pdp\frac{dN}{dp}, \tag{3}$$

and the harmonic flow coefficients

$$V_n = \frac{1}{N}\int_{p_{\min}}^{p_{\max}} dpV_n(p)\frac{dN}{dp}. \tag{4}$$

The complex numbers $V_n = v_n e^{in\Psi_n}$ describe the flow magnitude v_n and the flow angle Ψ_n for the harmonic flow of order n. The average over a sample of events in a given centrality bin is denoted by $\langle\cdots\rangle$, e.g., the averages of the multiplicity $\langle N\rangle$, transverse momentum $\langle p_T\rangle$, and flow harmonics

$$v_n\{2\} = \sqrt{\langle V_n V_n^\star\rangle} \tag{5}$$

can be calculated.

We use the two-dimensional version of the hydrodynamic code MUSIC [18–20] with shear viscosity $\eta/s = 0.08$ for the hydrodynamic expansion phase. For the initial conditions in Pb + Pb collisions at $\sqrt{s_{NN}} = 5.02$ TeV we use a two-component Glauber Monte Carlo model [21] to calculate the initial entropy density in each event. The details of the model for the initial density can be found in Ref. [5]. The initial density in the transverse plane $s(x, y)$ in each event can be characterized by specific moments, the eccentricities

$$\epsilon_n e^{i\Phi_n} = -\frac{\int r\,dr\,d\phi\, r^n s(r,\phi)e^{in\phi}}{\int r\,dr\,d\phi\, r^n s(r,\phi)}, \tag{6}$$

the RMS radius

$$R^2 = \frac{\int r\,dr\,d\phi\, r^2 s(r,\phi)}{\int r\,dr\,d\phi\, s(r,\phi)}, \tag{7}$$

and the entropy per unit rapidity,

$$S = \int r\,dr\,d\phi\, s(r,\phi). \tag{8}$$

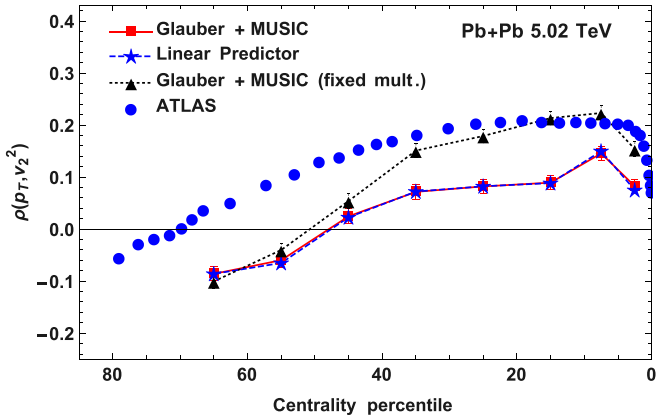

FIG. 1. The correlation coefficient of the average transverse momentum and the elliptic flow coefficient in Pb + Pb collisions as a function of centrality. The experimental data are from the ATLAS Collaboration [12] (blue points). The red squares denote the results of the hydrodynamic simulations, the black triangles show the results for the correlation coefficient corrected for multiplicity fluctuations (13), and the blue dashed line with stars shows the correlation coefficient obtained from the linear predictor (15).

B. Transverse momentum: Harmonic flow correlations

Event by event correlations between the average transverse momentum and the harmonic flow can be measured using the correlation coefficient [5]

$$\rho\left(p_T, v_n^2\right) = \frac{\mathrm{Cov}\left(p_T, v_n^2\right)}{\sqrt{\mathrm{Var}(p_T)\mathrm{Var}\left(v_n^2\right)}} \tag{9}$$

with the covariance

$$\mathrm{Cov}\left(p_T, v_n^2\right) = \langle p_T V_n V_n^\star\rangle - \langle p_T\rangle\langle V_n V_n^\star\rangle \tag{10}$$

and the variances

$$\mathrm{Var}(p_T) = \left\langle p_T^2\right\rangle - \langle p_T\rangle^2, \tag{11}$$

$$\mathrm{Var}\left(v_n^2\right) = \langle (V_n V_n^\star)^2\rangle - \langle V_n V_n^\star\rangle^2. \tag{12}$$

The covariance in the numerator of the correlation coefficient (9) is a three particle correlator, but the variance of the flow harmonic (12) is a four particle correlator. The experimental estimators for covariance and the variances in (9) involve up to three or four sums over particles in the event, with self-correlations excluded [5].

The results for the transverse momentum-elliptic flow correlation coefficient $\rho(p_T, v_2^2)$ are shown in Fig. 1. The simulated correlation coefficients present a qualitatively similar trend to the experimental data of the ATLAS Collaboration [12]. In particular, the correlation coefficient $\rho(p_T, v_2^2)$ decreases in the most central collisions, and in peripheral collisions the correlation coefficient changes sign.

It should be noted that the change of sign of $\rho(p_T, v_2^2)$ happens in the simulation for more central collisions than in the data. The measured correlation coefficient for the triangular flow $\rho(p_T, v_3^2)$ is small and is shown in Fig. 2. The simulation does not fully describe this feature of the experimental data. The discrepancies observed between the data and simulations

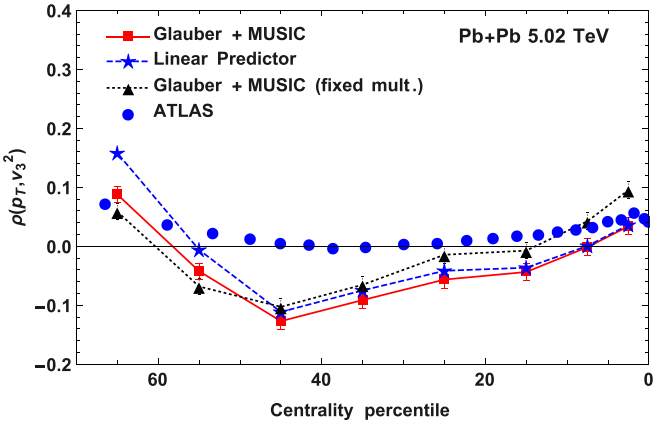

FIG. 2. Same as in Fig. 1, but for the triangular flow.

results for $\rho(p_T, v_n^2)$ may indicate that some physics of the dynamics in the model or some essential correlations in the initial state are missing. At very low multiplicities some correlations may be due to nonflow contributions and/or the initial flow, but it is difficult to explain why a significant discrepancy for $\rho(p_T, v_2^2)$ is visible also for mid-central collisions.

The correlation between the average transverse momentum and the flow harmonics is partially due to correlations of those quantities with the event multiplicity. The experimental data are presented in narrow bins of centrality, where this effect is reduced. The dependence of the variance or covariance of studied observables on the fluctuations of a third variable, e.g., the multiplicity, can be taken into account by calculating the partial variance or covariance [22]. The partial correlation coefficient

$$\rho\left(p_T, v_n^2 \bullet N\right) = \frac{\rho\left(p_T, v_n^2\right) - \rho(p_T, N)\rho\left(N, v_n^2\right)}{\sqrt{1-\rho(p_T,N)^2}\sqrt{1-\rho\left(v_n^2, N\right)^2}} \quad (13)$$

is an estimate of the correlation coefficient at fixed multiplicity [21]. The results for the partial correlation coefficients are shown in Figs. 1 and 2 (black triangles). The correction is sizable for the elliptic flow correlation coefficient $\rho(p_T, v_2^2)$. The partial correlation coefficient is closer to the experimental data. Generally, if the dependence of an observable O, in a given bin, on multiplicity is approximately linear, the correction to O can be implemented as [7]

$$\tilde{O} = O - \frac{\mathrm{Cov}(O,N)}{\mathrm{Var}(N)}(N - \langle N\rangle). \quad (14)$$

To correct for the effect of multiplicity fluctuation, we can calculate event averages for moments of the corrected variables (14). For the correlation coefficient this procedure is equivalent to the formula for the partial correlation coefficient (13). In the following, we use the corrected observables $\tilde{O}$ to estimate higher order cumulants without effects of multiplicity fluctuations. When comparing to the experimental data obtained in narrow multiplicity bins the simulation results corrected for multiplicity fluctuations should be considered. If the experimental data are obtained in wide multiplicity bins or using a different definition on centrality bins a correction similar to (14) could be used in order to obtain a consistent definition of correlations and cumulants between different experiments and model calculations.

C. Linear predictor

The average transverse momentum and the harmonic flow coefficients are largely determined by the initial conditions [4,23–25]. The eccentricities of the initial distribution are strongly correlated with harmonic flow coefficients of the emitted particles. The average transverse momentum of final particles can be predicted using the initial entropy S [Eq. (8)] and the RMS size R [Eq. (7)] [26,27]. Alternatively, a predictor of the final transverse momentum based on the initial energy per rapidity [8] or the energy weighted entropy [7] can be used.

It has been noted that in order to describe the correlation of the transverse momentum with the elliptic or triangular flow, the eccentricities should be included in the predictor for the final transverse momentum [6]. It was shown that such an improved predictor describes well the transverse momentum-harmonic flow correlation coefficients, obtained from the full hydrodynamic simulation. In the following we use a general linear predictor, based on moments of the initial density:

$$\begin{aligned}\hat{v}_2^2 &= k_2\epsilon_2^2 + \alpha_2\delta R + \beta_2\delta S,\\ \hat{v}_3^2 &= k_3\epsilon_3^2 + \alpha_3\delta R + \beta_3\delta S,\\ \hat{p}_T &= \langle p_T\rangle + \alpha_p\delta R + \beta_p\delta S + \gamma_p\delta\epsilon_2^2 + \lambda_p\delta\epsilon_3^2, \end{aligned} \quad (15)$$

where for any observable $\delta O = O - \langle O\rangle$. The prediction of each of the observables in the above equations is optimized separately. Only after fixing the parameters of the linear predictor, the cumulants between predicted observables are calculated. The linear predictor can be written as

$$\delta\hat{O}_i = L_i^j \delta M_j \quad (16)$$

with M_i being the set of moments of the initial density. The moments of the final observables can be written as a linear transformation from the moments in the initial state:

$$\langle \delta O_i \cdots \delta O_j\rangle = L_i^s \cdots L_j^k \langle \delta M_s \cdots \delta M_k\rangle. \quad (17)$$

The linear predictor (15) describes fairly well the correlations and higher cumulants involving p_T, v_2^2, and v_3^2 [compare blue stars (linear predictor) and red squares (hydrodynamic results) in Figs. 1, 2, 3, and 11]. It demonstrates that the proposed cumulants involving those observables can be understood as a linear hydrodynamic response on the correlations present in the initial state.

III. SYMMETRIC CUMULANTS

A. Second order cumulant

The correlation between the magnitudes of the harmonic flows of different order has been studied using symmetric cumulants [15]. The second order symmetric cumulant is the covariance between the two observables:

$$\langle AB\rangle - \langle A\rangle\langle B\rangle = \mathrm{Cov}(A,B). \quad (18)$$

The normalized symmetric cumulant (NSC) is scaled by the averages of the observables in the covariance. For the

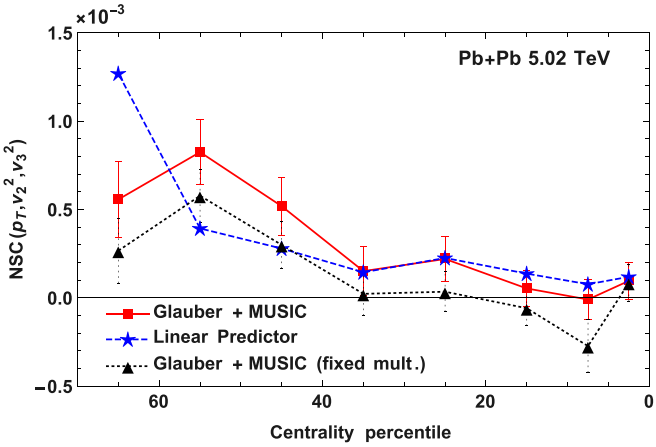

FIG. 3. The normalized symmetric cumulant of the average transverse momentum and the squares of the elliptic and triangular flow (red squares). The blue stars denote the results obtained from the linear predictor (15) and the black triangles show the scaled symmetric cumulant for observables corrected for multiplicity fluctuations (14).

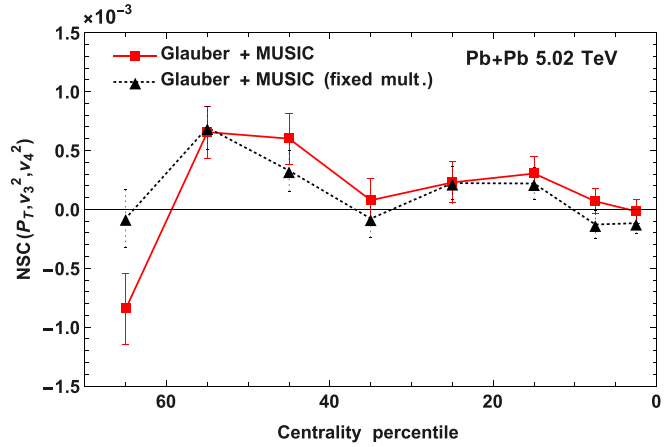

FIG. 4. Same as in Fig. 3 but for the triangular and quadratic flows.

transverse momentum and harmonic flow one may define

$$\mathrm{NSC}\left(p_T, v_n^2\right) = \frac{\langle p_T v_n^2\rangle - \langle p_T\rangle\langle v_n^2\rangle}{\langle p_T\rangle\langle v_n^2\rangle}. \tag{19}$$

The information on the event by event correlations between the average transverse momentum and the harmonic flow is contained in the covariance of the two observables, and is basically the same in the correlation coefficient $\rho(p_T, v_n^2)$ and in the symmetric cumulant $\mathrm{NSC}(p_T, v_n^2)$. The experimental extraction of the normalized symmetric cumulant is simpler than for the correlation coefficient, since the denominator involves at most a two particle correlator, where methods to reduce nonflow effects can be implemented, even in small collision systems [28].

B. Third and fourth order cumulants

Additional information on correlations between flow observables is encoded in higher order cumulants [15–17]. The nth order cumulant involves only correlation of n observables, with all lower order correlations subtracted. The third and fourth order symmetric cumulants for scalar observables have the form [16]

$$\begin{aligned}\mathrm{SC}(A,B,C) = {} & \langle ABC\rangle - \langle AB\rangle\langle C\rangle - \langle AC\rangle\langle B\rangle \\ & -\langle BC\rangle\langle A\rangle + 2\langle A\rangle\langle B\rangle\langle C\rangle \end{aligned} \tag{20}$$

and

$$\begin{aligned}\mathrm{SC}(A,B,C,D) = {} & \langle ABCD\rangle - \langle ABC\rangle\langle D\rangle - \langle ABD\rangle\langle C\rangle \\ & -\langle ACD\rangle\langle B\rangle - \langle BCD\rangle\langle A\rangle - \langle AB\rangle\langle CD\rangle \\ & -\langle AC\rangle\langle BD\rangle - \langle BC\rangle\langle AD\rangle + 2(\langle AB\rangle\langle C\rangle\langle D\rangle \\ & +\langle AC\rangle\langle B\rangle\langle D\rangle + \langle AD\rangle\langle C\rangle\langle B\rangle \\ & +\langle BC\rangle\langle A\rangle\langle D\rangle + \langle BD\rangle\langle A\rangle\langle C\rangle \\ & +\langle CD\rangle\langle A\rangle\langle B\rangle) - 6\langle A\rangle\langle B\rangle\langle C\rangle\langle D\rangle. \end{aligned} \tag{21}$$

The corresponding normalized symmetric cumulants are

$$\mathrm{NSC}(A,B,C) = \frac{\mathrm{SC}(A,B,C)}{\langle A\rangle\langle B\rangle\langle C\rangle} \tag{22}$$

and

$$\mathrm{NSC}(A,B,C,D) = \frac{\mathrm{SC}(A,B,C,D)}{\langle A\rangle\langle B\rangle\langle C\rangle\langle D\rangle}. \tag{23}$$

As noted, for higher order symmetric cumulants the effect of multiplicity fluctuations can be reduced using observables corrected for changes in multiplicity [Eq. (14)].

In Figs. 3, 4, and 5, the third order cumulants for p_T and two different coefficients of the harmonic flow are shown. For all the third order correlations considered, the magnitude of the scaled cumulant is small, as it measures only genuine third order correlations. For the cumulants $\mathrm{NSC}(p_T, v_2^2, v_3^2)$ and $\mathrm{NSC}(p_T, v_2^2, v_4^2)$ an increase is visible in peripheral collisions. The linear predictor (15), based on initial correlations only, describes the full hydrodynamic calculation for centralities 0–50%. The cumulants involving v_4 cannot be predicted using a linear predictor, but could serve as a precise measure of nonlinearities between harmonic flows of

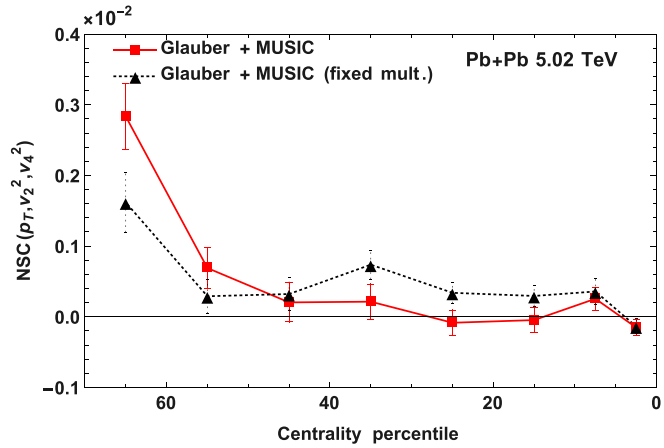

FIG. 5. Same as in Fig. 3 but for the elliptic and quadratic flows.

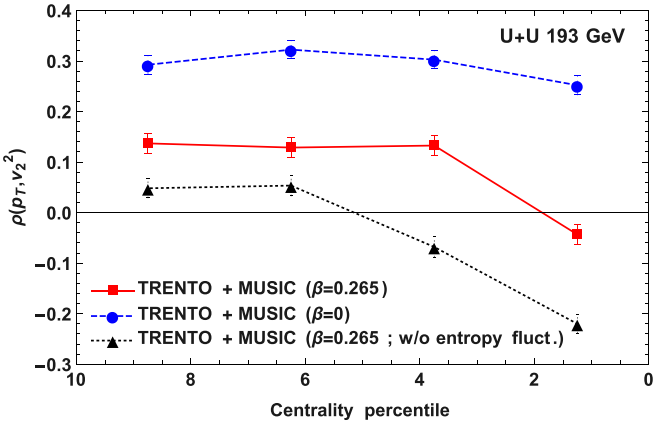

FIG. 6. The correlation coefficient between the average transverse momentum and the elliptic flow coefficient $\rho(p_T, v_2^2)$ for central U + U collisions at $\sqrt{s_{NN}} = 193$ GeV as a function of centrality. Results for collisions of deformed nuclei with and without fluctuations in entropy deposition are denoted with red squares and black triangles, respectively. The results for spherical nuclei are represented using blue dots.

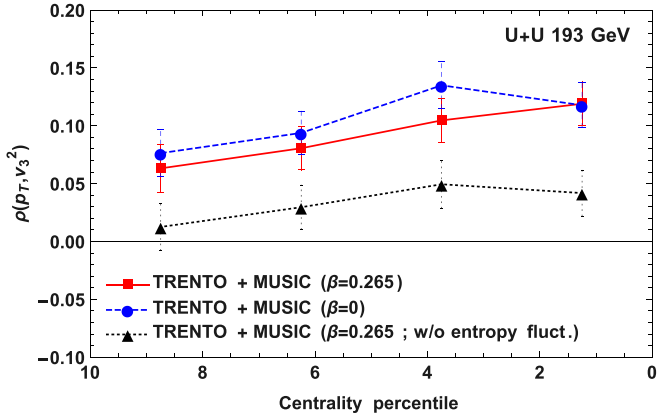

FIG. 7. Same as in Fig. 6 but for the triangular flow.

different order. The fourth order normalized symmetric cumulant NSC(p_T, v_2^2, v_3^2, v_4^2) is compatible with zero within the statistical accuracy of our calculation (not shown).

IV. SYMMETRIC CUMULANTS FOR COLLISIONS OF DEFORMED NUCLEI

In central collisions of deformed nuclei the relative orientation of the axes of deformation of the two nuclei determines the initial ellipticity, entropy, and the size of the fireball [11,29–34]. As a consequence, the final elliptic flow, the average transverse momentum, and/or the multiplicity may be correlated with the initial orientation of the deformation axes in a collision. In central collisions of deformed nuclei, tip-on-tip collisions lead to a large transverse momentum and small elliptic flow, while body-on-body collisions lead to a smaller transverse momentum but larger elliptic flow [10]. This effect reduces the value of the correlation coefficient $\rho(p_T, v_2^2)$ in central U + U collisions.

In this section symmetric cumulants for U + U collisions at $\sqrt{s_{NN}} = 193$ GeV are studied. Initial conditions from the TRENTO model (with parameter $p = 0$) [35] are evolved using the two-dimensional version of the MUSIC hydrodynamic code. We compare three scenarios for the initial conditions: collisions of uranium nuclei with deformation parameter $\beta = 0.265$ and fluctuations of entropy deposition from each participant (exponential distribution), collisions of spherical uranium nuclei ($\beta = 0$), and collisions of deformed uranium nuclei ($\beta = 0.265$) without fluctuations of entropy deposition. In Figs. 6 and 7, the correlation coefficients of the average transverse momentum and harmonic flow are shown. The value of the correlation coefficient $\rho(p_T, v_2^2)$ is smaller for collisions of deformed nuclei than in the case of spherical nuclei, as expected. We note that the correlation coefficient for initial conditions without fluctuations in entropy deposition is smaller than in the cases with fluctuations for both correlation coefficients $\rho(p_T, v_2^2)$ and $\rho(p_T, v_3^2)$. In central collisions, the covariances of the harmonic flow observables with multiplicity are small. We have checked that for the centrality bins used in our study for U + U collisions, the corrections for multiplicity fluctuations to the correlation coefficients and higher order symmetric cumulants are small. In the following we show only the uncorrected symmetric cumulants for U + U collisions. The third order symmetric cumulant NSC(p_T, v_2^2, v_3^2) is smaller for collisions of deformed nuclei with fluctuations of entropy deposition than in the other two scenarios studied (Fig. 8), but the effect is small.

The collective flow in central collisions of deformed nuclei is dominated by the fluctuations in the initial entropy and its azimuthal asymmetries. Therefore, it is interesting to study symmetric cumulants involving not only the average transverse momentum and harmonic flow, but also the multiplicity in the event. Please note that the results for the symmetric cumulants involving multiplicity as one of the

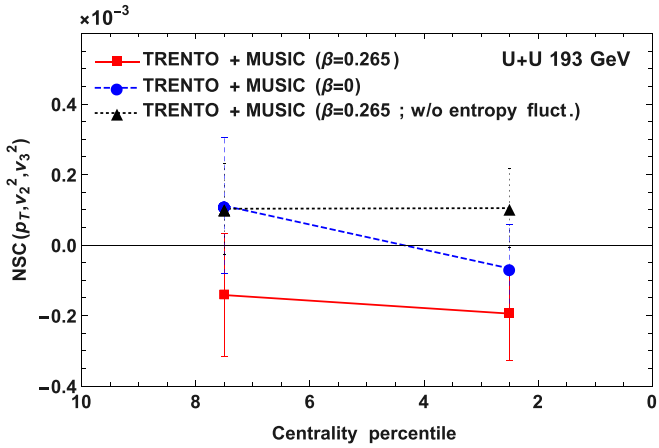

FIG. 8. The normalized symmetric cumulant of the average transverse momentum, the elliptic, and the triangular flow coefficients NSC(p_T, v_2^2, v_3^2) for central U + U collisions at $\sqrt{s_{NN}} = 193$ GeV as a function of centrality. Results for collisions of deformed nuclei with and without fluctuations in entropy deposition are denoted with red squares and black triangles, respectively. The results for spherical nuclei are represented using blue dots.

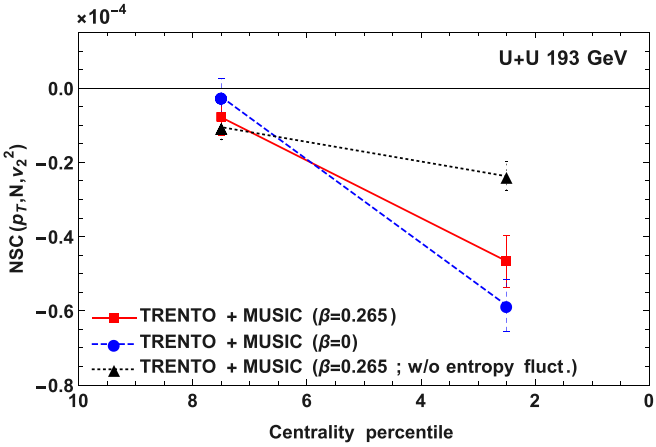

FIG. 9. Same as in Fig. 8 but for the normalized symmetric cumulant of the average transverse momentum, the multiplicity, and the elliptic flow coefficient NSC(p_T, N, v_2^2). Symbols as in Fig. 8.

observables may depend on the definition of the centrality bin. To reduce the bias from centrality cuts, that observables could be calculated experimentally using centrality bins based on forward rapidity observables, i.e., the forward transverse energy. The symmetric cumulant NSC(p_T, N, v_2^2) is sensitive to the fluctuations of entropy deposition from the participant nucleons (Fig. 9). Fluctuations in entropy deposition increase the magnitude of NSC(p_T, N, v_2^2). The fourth order cumulant NSC(p_T, N, v_2^2, v_3^2) is positive for simulations involving fluctuations in the entropy deposition in the initial states (Fig. 10), while it is compatible with zero for simulations without entropy fluctuations in the initial state. The normalized symmetric cumulant NSC(p_T, v_2^2, v_3^2, v_4^2) (not shown) is compatible with zero within our statistical accuracy.

V. SCALED SYMMETRIC CUMULANTS

The normalized symmetric cumulants (22) and (23) involve, in the denominator, averages of the observables for

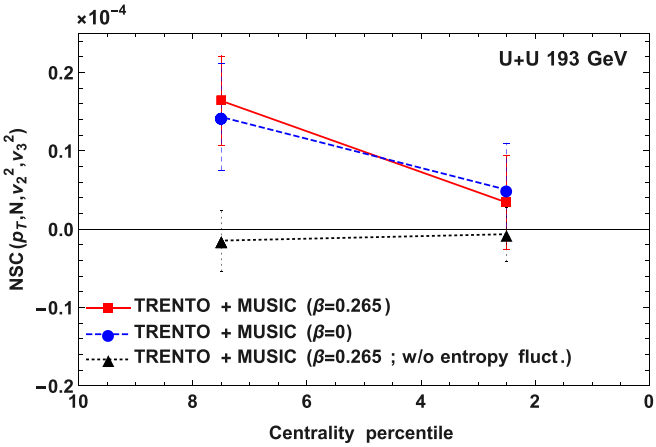

FIG. 10. The fourth order symmetric cumulant of the average transverse momentum, the multiplicity, the elliptic, and the triangular flow coefficients NSC(p_T, N, v_2^2, v_3^2). Symbols as in Fig. 8.

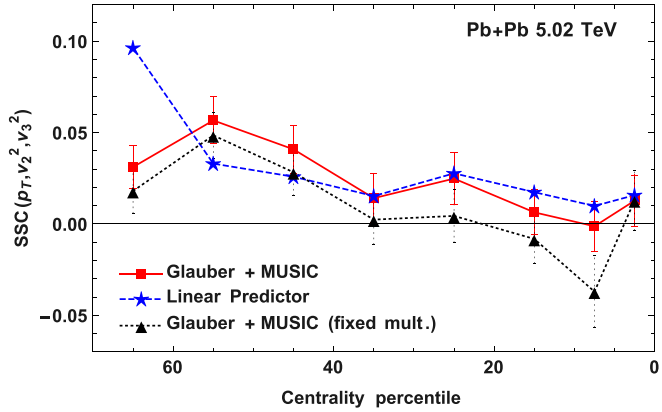

FIG. 11. The scaled symmetric cumulant of the average transverse momentum and the squares of the elliptic and triangular flow coefficients SSC(p_T, v_2^2, v_3^2) in Pb + Pb collisions as a function of centrality (red squares). The blue stars denote the results obtained from the linear predictor (15) and the black triangles show the scaled symmetric cumulant for observables corrected for multiplicity fluctuations (14).

which the cumulant is calculated. However, the interpretation of the results is less obvious than for the correlation coefficient. Moreover, the average transverse momentum in a collision depends on many effects [36]: the freeze-out procedure, the bulk viscosity, the pre-equilibrium flow, or simply the experimental transverse momentum range. The linear predictor for the average transverse momentum in an event (15) can predict only deviations from the mean.

An alternative normalization of the symmetric cumulants would involve the standard deviations of the observables in the denominator and we get the scaled symmetric cumulants (SSCs)_,

$$\mathrm{SSC}(A,B,C) = \frac{\mathrm{SC}(A,B,C)}{\sqrt{\mathrm{Var}(A)\mathrm{Var}(B)\mathrm{Var}(C)}} \tag{24}$$

and

$$\mathrm{SSC}(A,B,C,D) = \frac{\mathrm{SC}(A,B,C,D)}{\sqrt{\mathrm{Var}(A)\mathrm{Var}(B)\mathrm{Var}(C)\mathrm{Var}(D)}}. \tag{25}$$

The scaled symmetric cumulant has the advantage that its prediction from the initial state does not require additional input on the value of the average transverse momentum (from simulation or experiment). The value of the scaled symmetric cumulants can be fully predicted using the linear hydrodynamic response.

The scaled symmetric cumulants show a very similar behavior as the normalized symmetric cumulants discussed in previous sections. This can be seen in the examples chosen for Pb + Pb collisions (Fig. 11) and U + U collisions (Fig. 12). The numerical values are larger for the scaled symmetric cumulants than for the normalized symmetric cumulants. Alone the change from the normalization by the average transverse momentum to the normalization by its standard deviation yields a factor in the range 20–100.

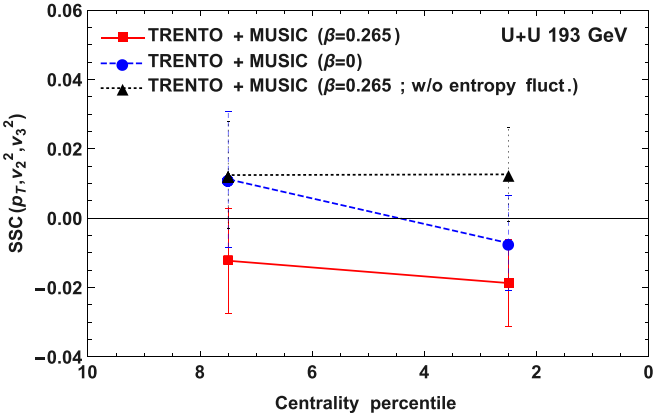

FIG. 12. The scaled symmetric cumulant of the average transverse momentum, the elliptic, and the triangular flow coefficients $\mathrm{SSC}(p_T, v_2^2, v_3^2)$ for central U + U collisions at $\sqrt{s_{NN}} = 193$ GeV as a function of centrality. Results for collisions of deformed nuclei with and without fluctuations in entropy deposition are denoted with red squares and black triangles, respectively. The results for spherical nuclei are represented using blue dots.

VI. SUMMARY

Flow observables are fluctuating from event to event. Moments from the values of several flow observables in the event can be constructed. We propose to measure higher order symmetric cumulants between the average transverse momentum and harmonic flow coefficients. Symmetric cumulants of order n measure genuine nth order correlations between the observables studied.

Symmetric cumulants can be normalized by the averages or by the standard deviations of the considered observables. Such normalized cumulants involving the elliptic flow, the triangular flow, and the transverse momentum could be predicted from the initial conditions. Their study could serve as a sensitive probe of higher order correlations in the initial state of the evolution in the collision. Further cumulants involving flow harmonics of higher order could serve as a probe of nonlinearities in the hydrodynamic response.

We present predictions based on the hydrodynamic model for collisions of spherical (Pb + Pb) or deformed (U + U) nuclei. The symmetric cumulants involving the elliptic and triangular flows obtained from the full hydrodynamic calculation can be well described using a linear predictor from the initial state. Our predictions could be compared to future experimental measurements.

ACKNOWLEDGMENTS

This research is supported by the AGH University of Science and Technology and by the Polish National Science Centre Grant No. 2019/35/O/ST2/00357.

[1] J.-Y. Ollitrault, J. Phys. Conf. Ser. **312**, 012002 (2011).
[2] U. Heinz and R. Snellings, Annu. Rev. Nucl. Part. Sci. **63**, 123 (2013).
[3] C. Gale, S. Jeon, and B. Schenke, Int. J. Mod. Phys. A **28**, 1340011 (2013).
[4] W. Broniowski, M. Chojnacki, and L. Obara, Phys. Rev. C **80**, 051902 (2009).
[5] P. Bożek, Phys. Rev. C **93**, 044908 (2016).
[6] P. Bożek and H. Mehrabpour, Phys. Rev. C **101**, 064902 (2020).
[7] B. Schenke, C. Shen, and D. Teaney, Phys. Rev. C **102**, 034905 (2020).
[8] G. Giacalone, F. G. Gardim, J. Noronha-Hostler, and J.-Y. Ollitrault, Phys. Rev. C **103**, 024909 (2021).
[9] G. Aad *et al.* (ATLAS Collaboration), Eur. Phys. J. C **79**, 985 (2019).
[10] G. Giacalone, Phys. Rev. Lett. **124**, 202301 (2020).
[11] G. Giacalone, Phys. Rev. C **102**, 024901 (2020).
[12] G. Aad *et al.* (ATLAS Collaboration), ATLAS-CONF-2021-001, 2021 (unpublished).
[13] J. Jia (STAR Collaboration), Sixth International Conference on the Initial Stages in High-Energy Nuclear Collisions, Revhovot (unpublished).
[14] G. Giacalone, B. Schenke, and C. Shen, Phys. Rev. Lett. **125**, 192301 (2020).
[15] A. Bilandzic, C. H. Christensen, K. Gulbrandsen, A. Hansen, and Y. Zhou, Phys. Rev. C **89**, 064904 (2014).
[16] C. Mordasini, A. Bilandzic, D. Karakoç, and S. F. Taghavi, Phys. Rev. C **102**, 024907 (2020).
[17] Z. Moravcova, K. Gulbrandsen, and Y. Zhou, Phys. Rev. C **103**, 024913 (2021).
[18] B. Schenke, S. Jeon, and C. Gale, Phys. Rev. C **82**, 014903 (2010).
[19] B. Schenke, S. Jeon, and C. Gale, Phys. Rev. Lett. **106**, 042301 (2011).
[20] J.-F. Paquet, C. Shen, G. S. Denicol, M. Luzum, B. Schenke, S. Jeon, and C. Gale, Phys. Rev. C **93**, 044906 (2016).
[21] P. Bożek, W. Broniowski, M. Rybczynski, and G. Stefanek, Comput. Phys. Commun. **245**, 106850 (2019).
[22] A. Olszewski and W. Broniowski, Phys. Rev. C **96**, 054903 (2017).
[23] F. G. Gardim, F. Grassi, M. Luzum, and J.-Y. Ollitrault, Phys. Rev. C **85**, 024908 (2012).
[24] Z. Qiu and U. W. Heinz, Phys. Rev. C **84**, 024911 (2011).
[25] H. Niemi, G. S. Denicol, H. Holopainen, and P. Huovinen, Phys. Rev. C **87**, 054901 (2013).
[26] A. Mazeliauskas and D. Teaney, Phys. Rev. C **93**, 024913 (2016).
[27] P. Bożek and W. Broniowski, Phys. Rev. C **96**, 014904 (2017).
[28] C. Zhang, A. Behera, S. Bhatta, and J. Jia, arXiv:2102.05200.
[29] U. W. Heinz and A. Kuhlman, Phys. Rev. Lett. **94**, 132301 (2005).
[30] A. Goldschmidt, Z. Qiu, C. Shen, and U. Heinz, Phys. Rev. C **92**, 044903 (2015).

[31] M. Rybczynski, W. Broniowski, and G. Stefanek, Phys. Rev. C **87**, 044908 (2013).
[32] M. R. Haque, Z.-W. Lin, and B. Mohanty, Phys. Rev. C **85**, 034905 (2012).
[33] S. Chatterjee and P. Tribedy, Phys. Rev. C **92**, 011902(R) (2015).
[34] L. Adamczyk *et al.* (STAR Collaboration), Phys. Rev. Lett. **115**, 222301 (2015).
[35] J. S. Moreland, J. E. Bernhard, and S. A. Bass, Phys. Rev. C **92**, 011901(R) (2015).
[36] P. Bożek and W. Broniowski, Phys. Rev. C **85**, 044910 (2012).